VIP Quadrupole Interactions

DOI: 10.1002/anie.201002860

Highly Specific Heterodimerization Mediated by Quadrupole Interactions**

*Hong Zheng and Jianmin Gao**

Specific protein–protein interactions serve as the basis of numerous biological processes, including gene expression regulation, signal transduction, and the assembly of molecular machineries. It has been a long-standing goal to decipher the molecular interactions that afford the exquisite selectivity between interacting proteins over highly analogous competitors. A great deal of effort has been paid to elucidate the role of polar interactions, including hydrogen bonding and salt bridges, as well as complementary hydrophobic groups. The knowledge learned enables the design of peptide assembly systems (for example peptide-based hydrogels and nanotubes), which hold great promise for applications in biotechnology and material science.[1] Presently, designed peptide-assembly systems largely rely on steric complementarity, hydrogen bonding, and salt bridges to control their structural specificity. Additional specificity elements will expand the modalities of molecular recognition and greatly increase the complexity of designed peptide assemblies that carry novel functions.

Aromatic and perfluoroaromatic compounds tend to associate with each other owing to the electrostatic attraction induced by their reversed quadrupoles.[2] For example, benzene and perfluorobenzene exhibit quadrupole moments of the same magnitude but with opposite signs (benzene $-29.0\times10^{-40}\,C\,m^{-2}$; perfluorobenzene $31.7\times10^{-40}\,C\,m^{-2}$). They mix readily to give a solid with a melting temperature higher than either of the components. The structure of the co-crystal reveals an alternating, stacked geometry with the aromatic faces parallel to each other.[3] The phenyl and perfluorophenyl pair can be easily incorporated into molecules of interest and has been widely used to afford specific molecular assemblies in solid state.[4] In contrast, few reports have investigated the potential of this supramolecular synthon in directing the folding and interaction of biopolymers. Two previous studies observed no advantage for a phenyl–perfluorophenyl pair to stabilize the helices of peptides and peptoids relative to a phenyl–phenyl pair.[5] The authors suggested that the stacking geometry of the aromatic rings might be prohibited in the helical structures. Herein, we document that, given the proper context, the quadrupole interaction of the phenyl–perfluorophenyl pair is strong enough to direct protein–protein interactions in aqueous media.

The designed protein α_2D was chosen as a tractable system for this investigation.[6] The 35-residue peptide folds as a homodimer and adopts a four-helix bundle structure (Figure 1a). The folding of α_2D is reversible and follows a

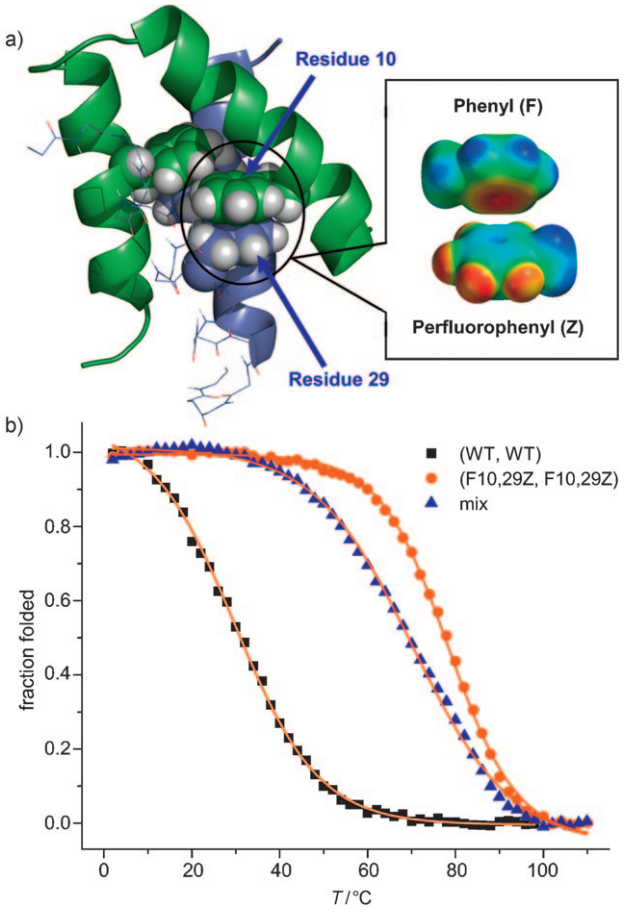

Figure 1. a) Representation of the dimeric structure of α_2D (PDB: 1QP6)[6] highlighting phenylalanines F10 and F29 in the stacking geometry. The monomers are colored green and blue, respectively. The front helix of the monomer in blue is omitted to make the aromatic cluster visible. Right: space-filling models of stacked side chains of F and Z, with the electrostatic potential mapped on their surface (blue: positive, red: negative). b) Thermal melting curves of the α_2D homodimers (WT, WT), (F10,29Z, F10,29Z), and the mixture of the two. The total peptide concentration was set to be 25 μM. Data was fitted into the two-state model.[7]

[*] H. Zheng, Prof. J. Gao
Department of Chemistry, Merkert Chemistry Center
Boston College
2609 Beacon Street, Chestnut Hill, MA, 02467 (USA)
E-mail: jianmin.gao@bc.edu
Homepage: http://www2.bc.edu/~gaojc/

[**] We thank the Smith Family Foundation and Boston College for financial support. We also acknowledge NSF (grant no. DBI-0619576) for providing the financial support of the BC Mass Spectrometry Center.

Supporting information for this article is available on the WWW under http://dx.doi.org/10.1002/anie.201002860.

two-state mechanism (unfolded monomer and folded dimer).[7] The hydrophobic core features an aromatic cluster, with the side chain of F10 from one monomer stacking against F29 from the other. Analyses of the sixteen low-energy conformers of the α_2D structure afford a centroid-to-centroid distance of 3.17 ± 0.14 Å and dihedral angles close to zero ($12 \pm 5°$) for the phenyl pair. Further molecular modeling shows that the edge-face geometry of the phenyl pair introduces steric clashes with the neighboring residues, thus it is unlikely to exist within the hydrophobic core of α_2D (Supporting Information, Figure S6).

Through the solid-phase peptide synthesis, we prepared the wild-type (WT) α_2D and also the double-mutant with pentafluorophenylalanines (named Z for brevity), which replaces both phenylalanines at positions 10 and 29. Both the WT and the mutant fold into stable helical structures, exhibiting the double-minima signature (208 and 222 nm) in their circular dichroism spectra (Supporting Information). Gel-filtration analyses confirm that the fluorinated peptide remains as a dimer: the folded F10,29Z elutes as a single peak with an essentially identical retention time as the WT, falling in between the two protein controls with molecular weights of 4.5 KDa and 13.7 KDa, respectively (Supporting Information, Figure S1). Given the molecular weight of about 4.3 KDa for the α_2D monomer, the gel-filtration result strongly indicates that the double-mutant retains the dimeric structure of the WT α_2D. For clarity, the homodimers are referred to as (WT, WT) and (F10,29Z, F10,29Z), respectively. We envisioned that mixing of the homodimers should give the heterodimer (WT, F10,29Z), in which side chains of F and Z engage in quadrupole interactions.

The α_2D variants were subjected to the thermal denaturation analysis. The melting curves of both peptides display cooperative two-state transitions. Interestingly, the fluorinated peptide exhibits greatly improved thermal stability, with a melting temperature of 79.8 °C in contrast to 29.8 °C for the WT α_2D at the same concentration (Figure 1b). More interestingly, the mixture of (WT, WT) and (F10,29Z, F10,29Z) at equal concentrations displays an apparent single transition instead of a two-stage profile expected for the sequential melting of (WT, WT) and (F10,29Z, F10,29Z). This observation supports our hypothesis that the F–Z stacking results in the formation of (WT, F10,29Z).

The heterodimer formation was further examined through a FRET (fluorescence resonance energy transfer) assay (Figure 2a). We chose to conjugate the fluorophores to the solvent exposed N-terminus of α_2D. The fluorescent labels are predicted to introduce little perturbation to the dimeric structure and stability. The WT and F10,29Z peptides were functionalized with nitrobenzofurazan (NBD) and tetramethylrhodamine (TAMRA) respectively. As expected, the fluorophore-labeled peptides fold into dimeric helical structures and display comparable T_m values as the corresponding unlabeled peptides (Supporting Information). With excitation at 460 nm, close to the absorption maximum of NBD, the NBD-labeled (WT, WT) displays a strong emission peaked at 540 nm, whilst the TAMRA-labeled (F10,29Z, F10,29Z) yields a weak emission at 587 nm (Figure 2b). Mixing the two homodimers at equal concentrations caused the complete

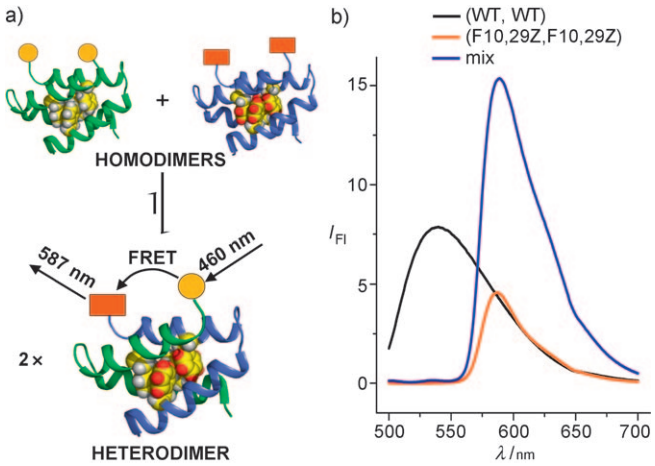

Figure 2. a) The FRET assay designed to examine the heterodimer formation between the WT α_2D and fluorinated variants. The WT and F10,29Z peptides are labeled with NBD (yellow circles) and TAMRA (red squares), respectively. b) The fluorescence emission data with excitation at 460 nm. The mixture displays a three-fold increase of the TAMRA emission and the complete disappearance of the NBD fluorescence, indicating formation of the heterodimer (WT, F10,29Z).

disappearance of the NBD fluorescence and a three-fold increase in TAMRA emission. Adding the NBD-labeled (WT, WT) into the solution of TAMRA alone resulted in no change in the fluorescence emission. Importantly, the gel-filtration analysis revealed that the mixture eluted as a single peak with an identical retention time as the homodimers (Supporting Information, Figure S1). Therefore, we attribute the fluorescence energy transfer to the heterodimer formation that brings NBD and TAMRA into proximity.

The heterodimerization process was also investigated by using NMR spectroscopy. The aromatic and amide regions of the ^{1}H NMR spectra for the two homodimers and their mixture are shown in Figure 3a. (F10,29Z, F10,29Z) exhibits much better dispersed signals than (WT, WT) as a consequence of its exceptionally high thermal stability. The N-H signals of Trp were easily identified owing to their exceptionally downfield chemical shifts, appearing at 9.85 ppm for (WT, WT) and 10.81 ppm for (F10,29Z, F10,29Z). The appearance of Trp N-Hs as a single peak is consistent with the homodimer structure in which the tryptophans (one from each monomer) reside in identical local environments. Mixing of (WT, WT) and (F10,29Z, F10,29Z) results in the complete disappearance of the signal at 9.85 ppm. Instead, the peaks at 10.85 and 10.90 ppm suggest the two tryptophans are placed in different local environments, as expected for the heterodimer (WT, F10,29Z).

Additional evidence for the heterodimer formation is obtained from the ^{19}F NMR data (Figure 3b). (F10,29Z, F10,29Z) exhibits four peaks with an integration ratio of 4:1:1:4. The peaks with the integration of 1 correspond to the *para* fluorine atoms of Z10 and Z29. The fluorine atoms at the *ortho* and *meta* positions each appear as a single peak with an integration of 4. Upon mixing with (WT, WT), the *ortho*-F and *meta*-F peaks each split into two with equal integration,

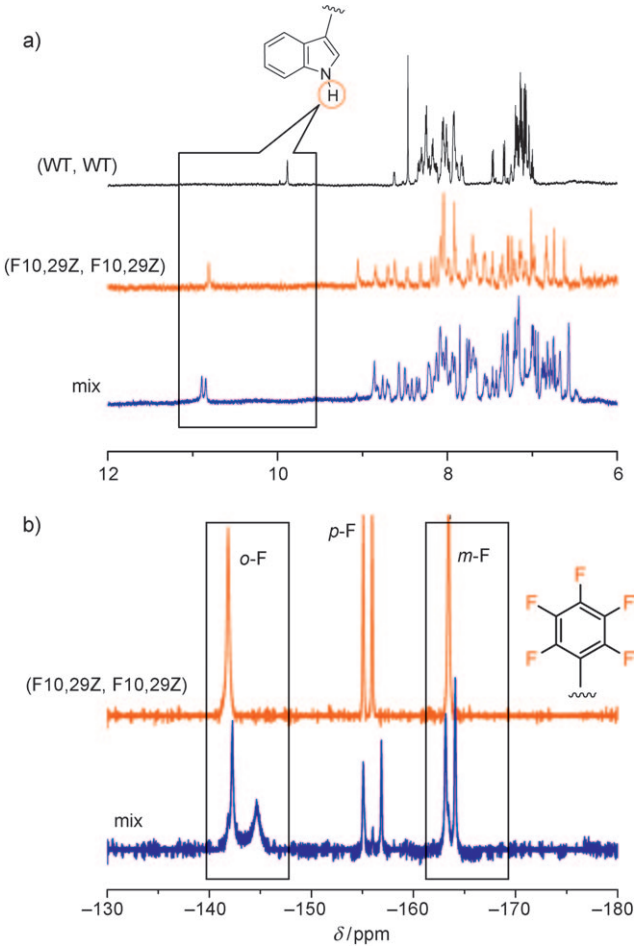

Figure 3. a) ^{1}H and b) ^{19}F NMR spectra of the α_2D homo/heterodimers. Mixing of the homodimers results in the downfield shift of the Trp N-H signal and the splitting of the *ortho* and *meta* fluorine signals. These data strongly support the formation of the (WT, F10,29Z) heterodimer.

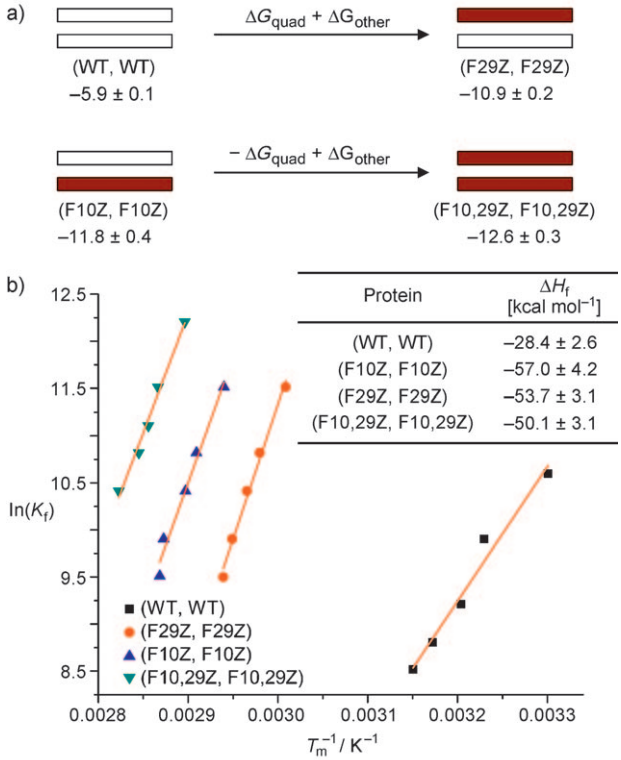

Figure 4. a) Double-mutant cycle of the α_2D variants to estimate the energetic scale of the F–Z quadrupole interaction. The stacked aromatic pairs in each protein variant are represented by two parallel rectangles, the open rectangles representing phenyl rings (the side chains of F) and the shaded ones representing perfluorophenyl rings (the side chains of Z). The folding free energies [kcal mol^{-1}] at 37 °C are listed under each protein variant. ΔG_{quad}: strength of the F–Z quadrupole interaction, ΔG_{other}: collective energetic contribution by other factors. b) The van't Hoff plots of the α_2D homodimers; linear fits yield the folding enthalpy (ΔH_f) values (table in inset).

indicating that the two Z side chains are placed into local contexts different from those of (F10,29Z, F10,29Z). Collectively, these results clearly show a heterodimer is formed, presumably as a consequence of the favorable F–Z quadrupole interaction.

To estimate the strength of the F–Z quadrupole stacking, we devised a double-mutant cycle (Figure 4a)[8] that consists of (WT, WT), (F10,29Z, F10,29Z), and two single-mutant dimers (F10Z, F10Z) and (F29Z, F29Z). Double-mutant cycles have been commonly used to analyze specific pairwise interactions. Starting with (WT, WT), the F-to-Z mutation at residue 29 stabilizes the dimeric structure by a number of noncovalent forces, including the F–Z quadrupole attraction. We dissect the total energetic gain of the F29Z mutation to the contribution of the quadrupole interaction (ΔG_{quad}) and that of other factors (ΔG_{other}). Such factors include hydrophobicity, steric effects, and possibly other weak interactions involving the C–F bonds[9] (see Supporting Information for details). Starting with the mutant (F10Z, F10Z), the F-to-Z mutation at residue 29 eliminates the favorable quadrupole interaction ($-\Delta G_{quad}$) and introduces the same energetic perturbation by other factors (ΔG_{other}). Based on these considerations, the value of ΔG_{quad} can be estimated based on the thermodynamic stabilities of the protein variants involved in the double-mutant cycle.

We attempted to quantify the folding free energies (ΔG_f) of the α_2D variants with guanidinium chloride (GdmCl) denaturation. However, these proteins were highly sensitive to chemical denaturants; no pre-transition baseline was observed, even in presence of 2 M TMAO (trimethylamine N-oxide), a well-established stabilizing osmolyte (Supporting Information).[10] Alternatively, thermodynamic parameters were deduced from the van't Hoff analysis of the thermal melting data at varied protein concentrations. Because of the homodimer fold, a more concentrated sample should yield a higher melting temperature. For each α_2D variant, thermal melting curves were recorded at five different concentrations. The van't Hoff analyses were carried out by plotting $\ln(K_f)$ against $1/T_m$ (Figure 4b). K_f is the association constant for α_2D dimerization at the corresponding T_m, which can be easily calculated from the total protein monomer concentration. The plots of $\ln(K_f)$ against $1/T_m$ fit a linear relationship well,

indicating that the heat capacity change (ΔC_p) of α_2D unfolding is rather minor. The folding enthalpy (ΔH_f) values were calculated based on the slopes of the linear fits of van't Hoff plots, which further yielded the folding free energies of the α_2D variants (see Supporting Information for details).

According to the double-mutant cycle, (F29Z, F29Z) is more stable than (WT, WT) by -5.0 ± 0.2 kcal mol^{-1}, which corresponds to the value of ($\Delta G_{quad} + \Delta G_{other}$). The double-mutant (F10,29Z, F10,29Z) is more stable than (F10Z, F10Z) by -0.8 ± 0.5 kcal mol^{-1}, corresponding to the value of ($-\Delta G_{quad} + \Delta G_{other}$). These data afford an estimation of -2.1 ± 0.6 kcal mol^{-1} for the total energetic gain owing to quadrupole stacking. Because the α_2D dimer structure consists of two F-Z pairs, each F-Z pair contributes -1.0 ± 0.3 kcal mol^{-1}. It is worth noting that a repulsive interaction may exist between a pair of stacking aromatic rings with quadrupole moments of the same sign. Therefore, the estimated value of ΔG_{quad} herein reflects the combined effect of eliminating the repulsive quadrupole interaction (between the F-F or Z-Z pairs) and introducing the attractive interaction of the F-Z pair. In other words, the ΔG_{quad} value should be considered as the upper limit of the quadrupole attraction between F and Z.

The estimated strength of the phenyl–perfluorophenyl quadrupole interaction agrees well with previously reported data based on the analysis of small molecules. By studying the rotational barriers of 1,8-diarylnaphthalenes, Siegel and co-workers showed the polar–π interaction between electron-rich and electronic-poor phenyl rings is worth about -1.0 kcal mol^{-1}.[11] A similar value was obtained by measuring benzene–perfluorobenzene association using NMR spectroscopy.[12] A slightly smaller value of -0.4 kcal mol^{-1} was reported by Adams et al. through analyzing the double-mutant cycles composed of hydrogen-bonded small molecule complexes.[13]

To the best of our knowledge, this report is the first estimate of the quadrupole attraction between the phenyl and perfluorophenyl groups in a protein context. Multiple reports in literature utilized the perfluorophenyl moiety in the design of enzyme inhibitors, which often yield better binding affinities.[14] However, the improved binding of the inhibitors reflects the collective consequence of the hydrophobic effect and electrostatic interactions, which could not be easily dissected. The same concern exists for a recent study that utilized the phenyl–perfluorophenyl pair to assemble collagen fibers.[15] The finding of this study complements the previous reports where no quadrupole contribution was observed to the stabilities of peptide/peptoid helices,[5] suggesting that quadrupole stacking may be best utilized to construct tertiary and quaternary structures where the stacking geometry is allowed.

In summary, we have shown that the quadrupole interaction between aromatic rings presents a significant driving force in directing selective protein–protein interactions. Even for simple aromatic structures, such as the phenyl–perfluorophenyl pair, the electrostatic attraction can contribute as much as -1.0 kcal mol^{-1} to protein structural stability and specificity. This energetic scale is comparable to that of weak hydrogen bonds.[16] We expect that the quadrupole interaction will supplement shape complementarity, hydrogen bonding, and salt bridges as a novel way of designing higher-order protein-assembly systems.

Received: May 12, 2010
Published online: August 2, 2010

Keywords: NMR spectroscopy · noncovalent interactions · peptide assembly · perfluorophenylalanine · protein–protein interactions

[1] a) E. H. Bromley, K. Channon, E. Moutevelis, D. N. Woolfson, *ACS Chem. Biol.* **2008**, *3*, 38; b) S. Cavalli, F. Albericio, A. Kros, *Chem. Soc. Rev.* **2010**, *39*, 241; c) M. C. Branco, J. P. Schneider, *Acta Biomater.* **2009**, *5*, 817.
[2] a) E. A. Meyer, R. K. Castellano, F. Diederich, *Angew. Chem.* **2003**, *115*, 1244; *Angew. Chem. Int. Ed.* **2003**, *42*, 1210; b) M. L. Waters, *Curr. Opin. Chem. Biol.* **2002**, *6*, 736.
[3] a) C. R. Patrick, G. S. Prosser, *Nature* **1960**, *187*, 1021; b) J. H. Williams, J. K. Cockcroft, A. N. Fitch, *Angew. Chem.* **1992**, *104*, 1666; *Angew. Chem. Int. Ed. Engl.* **1992**, *31*, 1655.
[4] a) M. Weck, A. R. Dunn, K. Matsumoto, G. W. Coates, E. B. Lobkovsky, R. H. Grubbs, *Angew. Chem.* **1999**, *111*, 2909; *Angew. Chem. Int. Ed.* **1999**, *38*, 2741; b) G. W. Coates, A. R. Dunn, L. M. Henling, J. W. Ziller, E. B. Lobkovsky, R. H. Grubbs, *J. Am. Chem. Soc.* **1998**, *120*, 3641; c) G. W. Coates, A. R. Dunn, L. M. Henling, D. A. Dougherty, R. H. Grubbs, *Angew. Chem.* **1997**, *109*, 290; *Angew. Chem. Int. Ed. Engl.* **1997**, *36*, 248; d) F. Ponzini, R. Zagha, K. Hardcastle, J. S. Siegel, *Angew. Chem.* **2000**, *112*, 2413; *Angew. Chem. Int. Ed.* **2000**, *39*, 2323; e) M. Gdaniec, W. Jankowski, M. J. Milewska, T. Polonski, *Angew. Chem.* **2003**, *115*, 4033; *Angew. Chem. Int. Ed.* **2003**, *42*, 3903; f) S. Bacchi, M. Benaglia, F. Cozzi, F. Demartin, G. Filippini, A. Gavezzotti, *Chem. Eur. J.* **2006**, *12*, 3538; g) F. Cozzi, S. Bacchi, G. Filippini, T. Pilati, A. Gavezzotti, *Chem. Eur. J.* **2007**, *13*, 7177.
[5] a) S. M. Butterfield, P. R. Patel, M. L. Waters, *J. Am. Chem. Soc.* **2002**, *124*, 9751; b) B. C. Gorske, H. E. Blackwell, *J. Am. Chem. Soc.* **2006**, *128*, 14378.
[6] R. B. Hill, W. F. DeGrado, *J. Am. Chem. Soc.* **1998**, *120*, 1138.
[7] D. P. Raleigh, S. F. Betz, W. F. Degrado, *J. Am. Chem. Soc.* **1995**, *117*, 7558.
[8] G. Schreiber, A. R. Fersht, *J. Mol. Biol.* **1995**, *248*, 478.
[9] a) J. A. Olsen, D. W. Banner, P. Seiler, U. Obst Sander, A. D'Arcy, M. Stihle, K. Muller, F. Diederich, *Angew. Chem.* **2003**, *115*, 2611; *Angew. Chem. Int. Ed.* **2003**, *42*, 2507; b) F. Hof, D. M. Scofield, W. B. Schweizer, F. Diederich, *Angew. Chem.* **2004**, *116*, 5166; *Angew. Chem. Int. Ed.* **2004**, *43*, 5056.
[10] C. C. Mello, D. Barrick, *Protein Sci.* **2003**, *12*, 1522.
[11] a) F. Cozzi, F. Ponzini, R. Annunziata, M. Cinquini, J. S. Siegel, *Angew. Chem.* **1995**, *107*, 1092; *Angew. Chem. Int. Ed. Engl.* **1995**, *34*, 1019; b) F. Cozzi, M. Cinquini, R. Annuziata, J. S. Siegel, *J. Am. Chem. Soc.* **1993**, *115*, 5330.
[12] R. Laatikainen, J. Ratilainen, R. Sebastian, H. Santa, *J. Am. Chem. Soc.* **1995**, *117*, 11006.
[13] H. Adams, J. L. J. Blanco, G. Chessari, C. A. Hunter, C. M. R. Low, J. M. Sanderson, J. G. Vinter, *Chem. Eur. J.* **2001**, *7*, 3494.
[14] a) C. Y. Kim, J. S. Chang, J. B. Doyon, T. T. Baird, C. A. Fierke, A. Jain, D. W. Christianson, *J. Am. Chem. Soc.* **2000**, *122*, 12125; b) V. M. Krishnamurthy, B. R. Bohall, C. Y. Kim, D. T. Moustakas, D. W. Christianson, G. M. Whitesides, *Chem. Asian J.* **2007**, *2*, 94; c) J. B. Doyon, E. A. Hansen, C. Y. Kim, J. S. Chang, D. W. Christianson, R. D. Madder, J. G. Voet, T. A. Baird, Jr., C. A. Fierke, A. Jain, *Org. Lett.* **2000**, *2*, 1189; d) B. C. Finzel, E. T.

Baldwin, G. L. Bryant, Jr., G. F. Hess, J. W. Wilks, C. M. Trepod, J. E. Mott, V. P. Marshall, G. L. Petzold, R. A. Poorman, T. J. O'Sullivan, H. J. Schostarez, M. A. Mitchell, *Protein Sci.* **1998**, *7*, 2118; e) A. Scozzafava, C. T. Supuran, *J. Med. Chem.* **2000**, *43*, 1858.

[15] M. A. Cejas, W. A. Kinney, C. Chen, J. G. Vinter, H. R. Almond, Jr., K. M. Balss, C. A. Maryanoff, U. Schmidt, M. Breslav, A. Mahan, E. Lacy, B. E. Maryanoff, *Proc. Natl. Acad. Sci. USA* **2008**, *105*, 8513.

[16] a) A. R. Fersht, J. P. Shi, J. Knill-Jones, D. M. Lowe, A. J. Wilkinson, D. M. Blow, P. Brick, P. Carter, M. M. Waye, G. Winter, *Nature* **1985**, *314*, 235; b) S. Deechongkit, H. Nguyen, E. T. Powers, P. E. Dawson, M. Gruebele, J. W. Kelly, *Nature* **2004**, *430*, 101.

